Tracking and Vertexing with a Thin CMOS Pixel Beam Telescope

Marco Battaglia [a,b], Dario Bisello [c], Gino Bolla [d], Daniela Bortoletto [d], Devis Contarato [b], Silvia Franchino [b,e], Piero Giubilato [b,c], Lindsay Glesener [a,b], Benjamin Hooberman [a,b] Devis Pantano [c],

[a] *Department of Physics, University of California at Berkeley, CA 94720, USA*
[b] *Lawrence Berkeley National Laboratory, Berkeley, CA 94720, USA*
[c] *Dipartimento di Fisica, Universita' di Padova and INFN, Sezione di Padova, I-35131 Padova, Italy*
[d] *Purdue University, Department of Physics, West Lafayette, IN 47907, USA*
[e] *Dipartimento di Fisica, Universita' di Pavia and INFN, Sezione di Pavia, I-35131 Pavia, Italy*

Abstract

We present results of a study of charged particle track and vertex reconstruction with a beam telescope made of four layers of 50 μm-thin CMOS monolithic pixel sensors using the 120 GeV protons at the FNAL Meson Test Beam Facility. We compare our results to the performance requirements of a future e^+e^- linear collider in terms of particle track extrapolation and vertex reconstruction accuracies.

Key words: Monolithic pixel sensor; Particle track and vertex reconstruction

1. Introduction

The physics program at a high energy linear e^+e^- collider, such as the ILC [1] or CLIC [2], relies significantly on the jet flavour tagging capability of its detectors. Distinguishing b, c and light quark jets as well as τ leptons is of prime importance both for extracting signals of new particles, which may couple preferentially to heavy fermions, and for analysing new sectors of particle physics, such as the Higgs mechanism. The identification of heavy quarks and leptons largely relies on their long lifetimes, which result in secondary and tertiary vertices separated from the beam interaction point by distances which range from few hundred microns to several millimetres, or even centimetres at multi-TeV collision energies. In order to efficiently identify these secondary vertices, it is essential to achieve excellent resolution on the extrapolation of charged particle tracks to their production point, $\sigma_{\rm extr}$. The requirement for a 0.5 TeV - 1.0 TeV linear collider has

been identified to be $\sigma_{\rm extr} = 5 \oplus \frac{10}{p_t}$ (μm), where p_t is the momentum component in the transverse plane, measured in GeV. These asymptotic and multiple scattering terms are respectively 3 and 8 times better than the design performance of the LHC detectors and 1.5 and 3 times better than the best extrapolation resolution ever achieved by a collider experiment detector, that of the VXD3 vertex detector in SLD at the Stanford Linear Collider [3]. Achieving these performances requires the development of novel sensor technologies. Monolithic silicon pixellated sensors, back-thinned to 20-50 μm have emerged as possibly the most appealing solution and a significant R&D effort is addressing various technologies and architectures in the framework of the world-wide linear collider studies. Small pixel size, fast readout and limited power dissipation, to enable airflow cooling and remove the material burden of active cooling, are some of the main issues being addressed. This R&D is guided by the physics requirements and detailed simulation studies of tracking performances. It is essential to validate these simulations with data collected from prototype trackers made of thin pixel sensors with a geometry resembling that envisaged for the ILC, under realistic operating conditions and hit occupancy levels.

In this paper we report the first results of the T966 beam test experiment at FNAL, which aims at a detailed study of tracking and vertexing capability of a prototype tracker based on thin CMOS monolithic Si pixel sensors.

2. The T966 Thin Pixel Telescope

The T966 beam test experiment took data at the Meson Test Beam Facility (MTBF) at FNAL in the Summer 2007 and deployed a beam telescope made of four layers of thinned CMOS pixel sensors. A prototype thin pixel telescope (TPPT-1) had been successfully operated on the 1.5 GeV BTS electron beam-line at the LBNL Advanced Light Source [4]. The T966 beam telescope has better mechanical positioning of the detector layers compared to the TPPT-1 condiguration and also includes remotely controlled stages for positioning a detector under test 20 mm downstream from the telescope and inserting a copper target $\simeq$ 30 mm upstream. The telescope consists of four detector layers, spaced 15 mm apart. This provides a geometry quite similar to that envisaged for the ILC Vertex Tracker, which has five to six sensitive layers spaced by $\simeq$ 11 mm, located at radii from 15 mm to 60 mm [5]. In particular, by extrapolating tracks reconstructed from hits on layers 2, 3 and 4 onto layer 1, we can study the extrapolation resolution for particle tracks over the same lever arm foreseen at the ILC, where the first layer of the Vertex Tracker would be positioned $\simeq$ 15 mm away from the beam interaction point.

The telescope uses the MIMOSA-5 chip, developed by IPHC, Strasbourg (France) [6,7]. This chip, fabricated in the AMS 0.6 μm process, features a large active area of 1.7×1.7 cm^2 and more than 1 Million pixels, arranged in four independent sectors. The epitaxial layer is 14 μm thick and the pixel size 17×17 μm^2. Detectors have been thinned by Aptek Industries [8] to (50 ± 7) μm using a proprietary grinding process. Each detector is glued to a PC board using a precision mounting jig which ensures a position accuracy of the detector corners w.r.t. the boards of $\simeq$ 20 μm. The board has a cut-out area corresponding to the sensor sensitive region to reduce multiple scattering. We verify the flatness of the thin chips after gluing them on the PC board using an optical survey system which has a resolution of $\simeq$ 1 μm. We measure the deviation between the height of 100 points on the chip surface and that of a plane interpolated through them. This has a Gaussian width of

7 μm. The PC boards are mounted on the readout board and held in place by precision mechanics which ensures their relative alignment. We verify the stability by measuring fiducial reference marks on the four PC boards before and after mechanically disturbing the setup. From these measurements we estimate that the sensitive area of each layer is stable within ≤ 20 μm in the z coordinate, along the beam axis, and ≤ 10 μm in the x and y coordinates, transverse to it. The telescope and its readout electronics are installed in an optical enclosure. The system is aligned on the beam-line using a laser beam and is operated at a constant temperature of +20°C, by flowing cold air inside the optical enclosure. The temperature is monitored by a thermocouple installed between layer 2 and 3 of the telescope.

One sector of each chip, corresponding to a 510×512 pixel array, is read out through a custom FPGA-driven acquisition board. The trigger is provided by two finger scintillators, S1 and S2, mounted just in front of the optical enclosure, defining a fiducial area of $\simeq$1 cm^2 around the sector of the MIMOSA chip that is readout. The S1-S2 coincidence is gated on the 4 s-long spill extraction signal. The readout cycle consists of a reset followed by the readout of two subsequent frames of the 510×512 pixel sector. The chip is read out at 3.125 MHz, which corresponds to 84 ms for reading a full sector. Four 14 bits, 40 MSample/s ADCs simultaneously read the four sensors, while an array of digital buffers drives all the required clocks and synchronisation signals. The FPGA has been programmed to generate the clock pattern and collect the sampled data from the ADCs. A 32 bit wide bus connects the FPGA to a digital acquisition board installed on a control PC. Due to the slow readout and data transfer, the telescope acquires 7 to 10 events/spill. Data are processed on-line by a LabView-based program, which performs correlated double sampling and pedestal subtraction, noise computation and cluster identification. To reduce the amount of data written to disk, only the addresses and pulse heights of the pixels in a fixed matrix around the centre of a cluster candidate having a seed pixel with signal-to-noise ratio above 4 are recorded. Data are converted offline in the `LCIO` format [9] for the subsequent analysis.

The average pixel noise has been measured to be (85 $\pm$ 16) e^- of equivalent noise charge (ENC), which is due both to the noise of the readout electronics and to leakage current from operating the detector at +20°C. A test performed in the lab shows that the noise drops to $\simeq$ 50 e^- of ENC, when operating the detector below +5°C.

During the 2007 data taking, the 120 GeV proton beam was extracted from the Main Injector and attenuated through a pinhole collimator. The average beam size was measured to be about 4 mm and 9 mm in the horizontal and vertical coordinate, respectively, using two sets of multi-wire chambers located upstream from the telescope. The average beam divergence, measured from the slope of tracks reconstructed in the telescope, is 0.52 mrad. The beam intensity was varied during data taking and resulted in an average hit density ranging from 0.07 hits mm^{-2} to 0.70 hits mm^{-2}, with local densities of up to 5 hits mm^{-2}. For comparison, in the core of hadronic jets from e^+e^- collisions, the average hit density is expected to be in the range 0.2-1.0 hits mm^{-2} for $\sqrt{s}$=0.5 TeV and 0.5-2.5 hits mm^{-2} for 3.0 TeV [10]. The machine-induced pair background contributes $\simeq$0.05 hits mm^{-2} bunch crossing^{-1} at 15 mm radius at 0.5 TeV [11,5] and $\simeq$0.005 hits mm^{-2} bunch crossing^{-1} at 30 mm radius at 3.0 TeV [2] for solenoidal fields of 4 T and 5 T, respectively. Local densities up to 5 hits mm^{-2} are quite comparable to those expected in a linear collider vertex tracker. At the same time our redundancy is lower than that provided by a five-layered vertex tracker and a main tracker, which

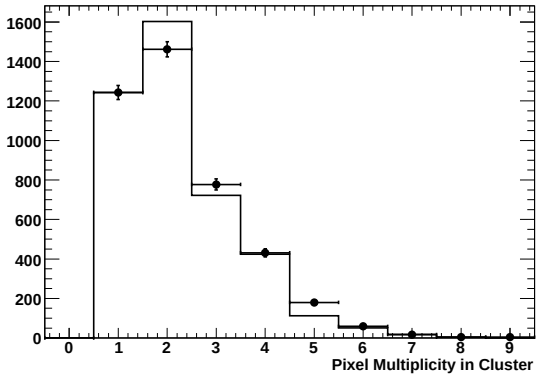

Fig. 1. Pixel multiplicity for clusters associated to a particle track. Data are shown as points with error bars and simulation with the histogram.

makes the overall occupancy conditions quite realistic.

3. Reconstruction and Simulation

The offline analysis is performed using a set of dedicated processors developed for the `Marlin` framework [12]. Individual processors are used for clustering and hit reconstruction, pattern recognition and track fit and for vertexing. An additional processor provides signal simulation of the pixels. The T966 setup is modelled by a simulation program based on the `Geant-4` package [13], which generates particle points of impact and energy deposits in the sensitive detector planes and accounts for the material surrounding the beam-line and the detectors. Simulated data are stored in `LCIO` format and used as input to the CMOS pixel simulation processor, `PixelSim`, implemented in `Marlin` [14].

Hits are reconstructed from the recorded pixel pulse heights as follows: each detector is scanned for pixels with pulse height over a given signal-to-noise (S/N) threshold. These are designated as cluster 'seeds'. Seeds are then sorted according to their pulse height values and the surrounding, neighbouring pixels are tested for addition to the cluster. The S/N threshold is 5 for the seed pixel and 2.5 for the neighbour pixels. The neighbour search is performed in a 5×5 matrix. Clusters are not allowed to overlap, i.e. pixels already associated to one cluster are not considered for populating another cluster around a different seed. Finally, we require that clusters are not discontinuous, i.e. pixels associated to a cluster cannot be interleaved by any pixel below the neighbour threshold. Pixels with noise exceeding two times the average sector noise or giving a pulse height above the seed threshold in more than 10 % of the events of a given run are flagged as noisy and removed offline for the whole run. Columns of pixels with more than 25 pixels having pulse height above the seed threshold in one event are also flagged as noisy and removed for that single event. Selected clusters have an average pixel multiplicity of 2.35 and average signal-to-noise ratio of 10.3. These results are in agreement with those predicted by simulation, as shown in Figure 1. Simulation predicts single point resolutions, $\sigma_{\rm point}$, of (2.90±0.02) μm, (2.08±0.02) μm and (1.70±0.02) μm for cluster S/N values of 10, 15 and 20. This last value agrees with the resolution of 1.7 μm, reported in [6], obtained by operating the detector cold. The track reconstruction efficiency is

estimated using simulation where the noise of each individual layer is tuned on the data. Particle densities comparable to those registered in the data are simulated and pixels are masked to reproduce the effect of noisy pixels and columns. Simulation reproduces well the number of reconstructed particles and the number of associated hits. Due to the limited pixel S/N performance achieved in our 2007 data taking, the estimated track reconstruction efficiency, after applying the full set of selection criteria as in real data, is 0.69.

4. Alignment

The relative position of the four layers of the telescope is obtained by using the result of an optical survey and a track-based alignment procedure to align the telescope planes with respect to a common reference system. The origin of this system coincides with the centre of the detector chip in the first layer and the x and y directions are aligned along the pixel rows and columns in their readout direction. For each telescope layer we consider six degrees of freedom: the three offsets along the x, y and z axes and the three rotations around them. These parameters are determined from a χ^2 fit which minimises the distance between the hit positions measured on each plane and those predicted by the extrapolation from the other planes. The optical survey provides with the starting positions. The track-based alignment procedure aligns the detector planes in pairs. We start with aligning the second telescope plane with respect to the first. The third plane is then aligned on the extrapolated positions determined from the track segments fitted with the first two planes. Finally, the fourth sensor is aligned with respect to the tracks obtained from a linear fit between the first three telescope planes. After this initial procedure, any given plane can be re-aligned on the extrapolations of the tracks fitted with the other three planes. Quality cuts are applied on the track slopes and fit χ^2. Due to a $\simeq$ 5-9°C difference in temperature between the day, when the telescope is operated, and the night, when its power is switched off, the procedure is repeated for each day of data taking, in order to account for possible distortions due to thermal effects. Changes in the relative position of the layers of up to 6-7 μm are observed, as shown in Figure 2. This result is consistent with the measured stability of the mechanical mounting. A sub-micron accuracy on the relative position of any pairs of layers is obtained with samples of $\leq$ 250 fitted tracks. These results are relevant for estimating the amount of data needed for aligning a single ladder in a full Vertex Tracker at a collider. Alignment parameters are stored in a conditions database using the Linear Collider Conditions Data (`LCCD`) toolkit [12], a C++ based `LCIO` framework. `LCCD` offers the advantage of full database functionality while being straightforward and easy to implement. Conditions data consisting of a set of alignment parameters for each day of data taking are stored in an `LCIO` file and are accessed by a `Marlin` module at run time.

5. Tracking Results

Particle tracks are fitted using the reconstructed hits with a simple straight track model. The pattern recognition starts from hits on a given detector layer and looks for sets of aligned hits. Hit pairs are used as track seeds provided the slope does not exceed 0.0015. Additional hits are tested if their residual w.r.t the track extrapolation does not

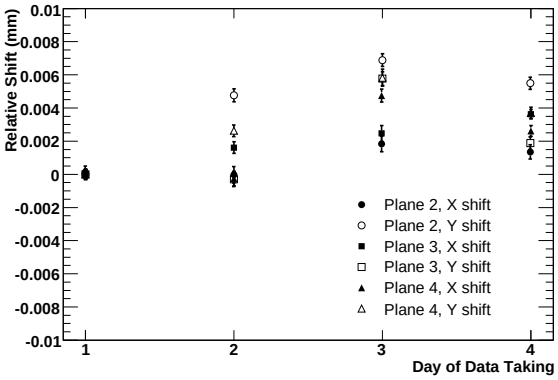

Fig. 2. Relative position of the telescope layers w.r.t. the first layer as a function of day of data taking as obtained from the track alignment.

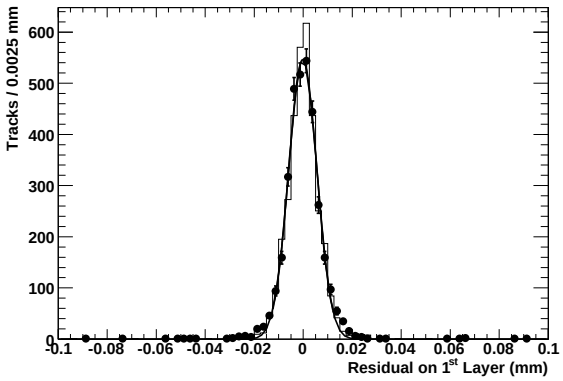

Fig. 3. Residual between the track extrapolation and the position of the closest hit on the first layer of the telescope. Data are shown as points with error bars and simulation by the histogram. The Gaussian curve fitted to the data has a width of 5.7 μm.

exceed 35 μm. Hit bundles corresponding to the χ^2 minimum for a given hit on the starting layer are used to define a track candidate provided that $\chi^2 < 25$ and the slope does not exceed 0.0010. The slope cut removes lower momentum particles originating from interactions and scattering upstream in the beamline as well as badly reconstructed particle tracks resulting from pattern recognition failures. The procedure is repeated using all planes. Ambiguities in hit association are then resolved based on the number of hits in a track candidate and its fit χ^2. Tracks are fitted and associated hits are flagged. The remaining unassociated hits are used for a second pass pattern recognition, where three- and two-hit tracks are reconstructed from the hit combinations giving the minimum χ^2 provided they do not exceed 25 or the minimum slope, respectively. The procedure is tested on simulated events with the same track density as the data. The fraction of correctly associated hits is 0.93 ± 0.01 for tracks with at least three hits. Residuals are computed from the distance between the track extrapolation on a test detector plane and the closest hit, which is not included in the track fit. Only tracks having an associated hit on the layer closest to the extrapolation plane are considered. First we determine

the detector single point resolution by including the hits on all four telescope layers in the track fit. Using the fact that the layers are equally spaced, we can extract the single point resolution $\sigma_{\rm point}$ from the width of the measured residual distribution, corrected by a geometrical factor, under the assumption that $\sigma_{\rm point}$ is the same for all layers. We measure a Gaussian width of (1.57±0.02) μm and (1.26±0.10) μm using hits from clusters with an average S/N ratio of 10 and 15, respectively. Using the correction factor of 1.81 for our geometry, we obtain an estimate of $\sigma_{\rm point}$ = (2.85±0.04) μm and (2.29±0.18) μm for cluster hits with average signal-to-noise ratio of 10 and 15, respectively. This result is in good agreement with the prediction of our CMOS sensor simulation, as discussed above. Then we extrapolate the tracks on the second layer and study the distribution of the residuals between the position of extrapolated and that of the closest hit, which is not included in the track fit. This distribution has a Gaussian width of (4.6±0.2) μm for data and (4.1±0.2) μm for simulation, for an average cluster S/N ratio of 10.3. Finally, we study the residuals obtained by extrapolating the track 15 mm upstream onto the first telescope layer, which resembles the extrapolation of a particle track back to its production point. This has a Gaussian width of (5.7±0.1) μm while simulation predicts (5.6±0.1) μm as shown in Figure 3. In order to measure the dependence of these residuals on the S/N ratio of the hit clusters, we vary the threshold on the seed pixel S/N ratio of all associated hits and compute the r.m.s. width of the residual distribution on the first layer as a function of the average S/N ratio of the hits on a track. Results are shown in Figure 4 for data and simulation. We also evaluate the effect of hit density on the non-Gaussian tails of the residual distribution. The fraction F of tracks with a residual on the first layer, which is more than 2.5 σ away from zero, is studied as a function of the minimum distance, $d_{\rm ch}$, between the hits associated to the track and the closest, not associated hit on any of the layers 2, 3 and 4. The most probable value of this distance in data is 0.19 mm. As a comparison, in the core of a b jet from $e^+e^- \rightarrow Z^0H^0$, $H^0 \rightarrow b\bar{b}$ at 0.5 TeV, disregarding the machine-induced pair background, the most probable value of d_{ch} is 0.40 mm. The fraction F is 0.040, for data where the distance $d_{\rm ch}$ is larger than 100 μm, and increases to 0.050 and 0.085, when $d_{\rm ch}$ drops below 100 μm and 75 μm, respectively. This trend is consistent with that predicted by simulation and gives a measure of the rate of outliers in the pattern recognition in presence of large hit occupancy. The extrapolation resolution on the first layer can be extracted from the measured width of the residual distribution by subtracting in quadrature the detector resolution, taken from simulation. This gives an extrapolation resolution of $\sigma_{\rm extr}$=(4.9±0.1) μm and (4.2±0.3) μm for cluster S/N values of 10 and 15, respectively. In an earlier paper, we reported the measurement of the extrapolation resolution for 1.5 GeV electrons, where we obtained $\sigma_{\rm extr}$=(8.5±0.4) μm with the TPPT-1 telescope [4]. These results are now compared in Figure 5 to the required track extrapolation resolution for e^+e^- collisions at 0.5 TeV at the ILC. These data reaches the target performance required for the ILC, using a standalone Si pixel tracker of similar geometry to that proposed for an ILC detector, in a high density track environment and rather realistic operating conditions with airflow cooling.

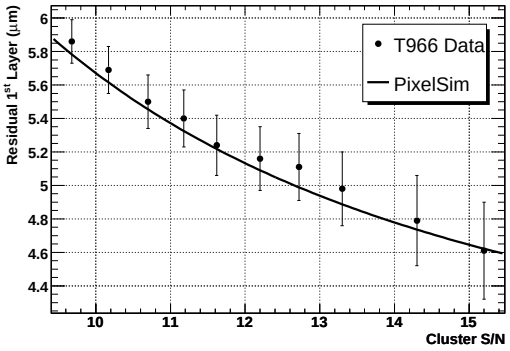

Fig. 4. Gaussian width of the distribution of residual between track extrapolation and position of closest hit on the first layer of the telescope as a function of the average S/N of the hit clusters used for reconstructing the track. Data are shown as points with error bars and simulation by the continuous line.

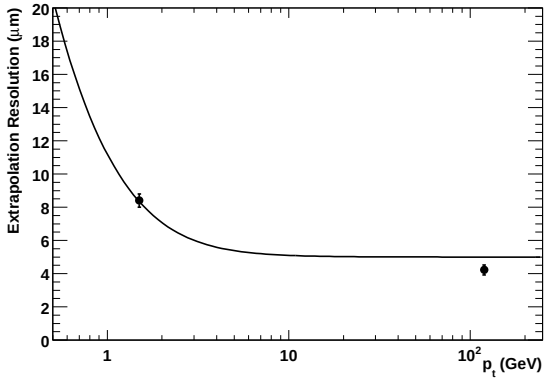

Fig. 5. Track extrapolation resolution, $\sigma_{\rm extr}$, as a function of the particle momentum. Data at 1.5 GeV and 120 GeV are shown as points with error bars and the $5 \oplus \frac{10}{p_t}$ (μm) requirement as a continuous line.

6. Vertexing Results

A set of data has been taken with a 4 mm thick Cu target inserted on the beamline, $\simeq$ 30 mm upstream of the first beam telescope plane. These data are used to collect inclined tracks, from protons scattered in the target, for alignment purposes as well as for a first study of vertex reconstruction performance with a thin pixel tracker telescope in 120 GeV p-Cu interactions. For this study we relax the requirement on the minimum S/N ratio of the seed pixel in the cluster to 4 and we raise the maximum track slope to 0.0085. Vertices are fitted using a port to the `Marlin` framework of the `VT` [15] Kalman filter vertex fitter, developed for HERA-B and LHCb, according to the following procedure. First a seed vertex is searched for. This is defined as a vertex made of a pair of tracks with at least three associated hits, including one on the first layer, and having a slope in excess of 0.00075. These cuts suppress combinatorics due to either fake tracks or primary protons not interacting with the target and have been optimised using fully simulated and

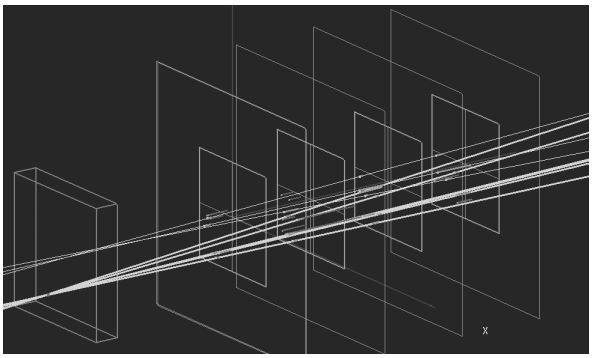

Fig. 6. Display of one of the largest multiplicity interaction events: a reconstructed six-prong vertex from the interaction of an 120 GeV proton in the Cu target.

reconstructed p-Cu interaction events. Seeds with a fit χ^2 below 20 are kept. Additional tracks are tested for association with this seed vertex. Tracks are retained if their χ^2 contribution does not exceed 10 and the vertex position along z does not change by more than five times the estimated uncertainty. Finally, unassociated hits are tested for their compatibility with this vertex. A track search is performed using the seed vertex as a track point. Tracks reconstructed with at least two associated hits, $\chi^2 < 15$ and slope below 0.0100 are accepted. The vertex is then refitted using all associated tracks. Vertices with χ^2/n.d.o.f. < 2.5 and at least one track with slope in excess of 0.010 are kept. The distribution of the reconstructed vertex positions along the beam axis, z, shows a clear accumulation at the target location. An event with a reconstructed six-prong vertex in the target is shown in Figure 6. The analysis has been applied to both simulated events, where a comparable number of protons per event collide against a copper target as in the actual data, and to data taken without the target in front of the telescope. These data are used as a control sample to estimate the background from combinatorics. The data control sample has a flat distribution of the z position of the reconstructed vertices, consistent with the sidebands of the data target sample (see Figure 7). The number of tracks associated to these vertices in data agrees with that predicted by simulation for real vertices (see Figure 7). The average multiplicity of tracks at the vertex is 2.74±0.09 in background-subtracted data and 2.73±0.04 in signal simulation.

Finally, we study the distribution of the resolution on the vertex position along the particle line of flight. The estimation of the resolution is validated using simulated events. The z pull distribution, i.e. the difference between the simulated and reconstructed z positions normalised to their estimated uncertainty, has a Gaussian width of 1.03±0.05. The average resolution in data is (260±10) μm for vertices $\simeq$32 mm away from the first sensitive layer. This can be compared to the resolution obtained for B decay vertices in simulated b jets at the ILC, which are $\simeq$15 mm away from the first sensitive layer. Simulated vertices from B mesons with energies in the range 100 GeV-150 GeV, re-weighted by the associated track multiplicity to match that of the reconstructed vertices in our data, have a resolution of (170±20) μm.

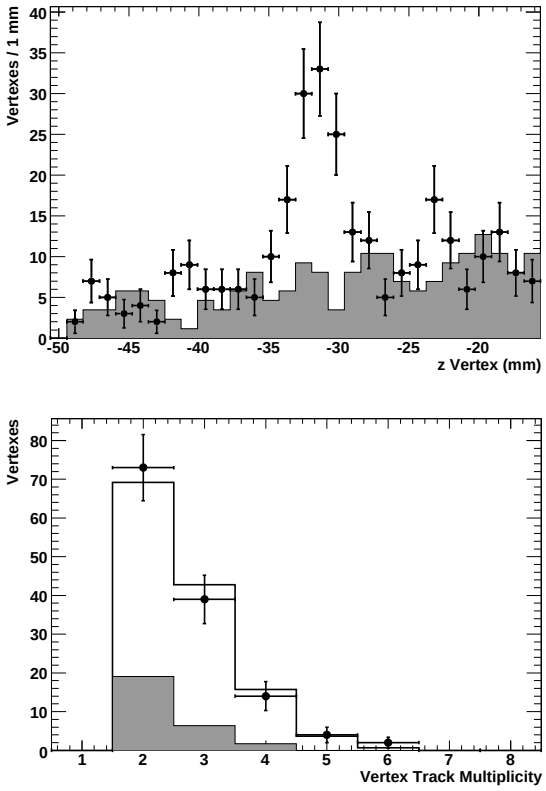

Fig. 7. Vertex reconstruction for p-Cu interaction events: (above) reconstructed vertex position along the beam axis, z, and (below) multiplicity of tracks associated to a reconstructed vertex. Data are shown as points with error bars and simulation with the open histogram, while the grey filled histogram gives the distribution from combinatorial background from events taken without target, rescaled to the same number of analysed events as those with the target.

7. Conclusions

The analysis of the data collected in the first run of the T966 beam test experiment at FNAL MTBF with a beam telescope based on thin monolithic CMOS pixel sensors has provided information on tracking and vertexing capabilities in rather realistic conditions. The resolution for extrapolating tracks 15 mm upstream of the first telescope plane is measured to be 4.2 μm to 4.9 μm, depending on the S/N of the hit clusters used for reconstructing the tracks. Vertices from 120 GeV p-Cu interactions have been reconstructed with a resolution of (260$\pm$10) μm along the flight direction.

Acknowledgements
This work was supported by the Director, Office of Science, of the U.S. Department of Energy under Contract No.DE-AC02-05CH11231. We are indebted to E. Ramberg and

the Main Injector staff for their assistance and the excellent performance of the machine and to FNAL for hospitality. We gratefully acknowledge the contribution of I. Childres, K. Deck and M. Marins De Castro Souza to the data taking and data quality checking.

References

[1] A. Djouadi, J. Lykken, K. Monig, Y. Okada, M. J. Oreglia and S. Yamashita (Editors), *International Linear Collider Reference Design Report*, Volume 2: *PHYSICS AT THE ILC*, arXiv:0709.1893 [hep-ph].
[2] M. Battaglia, A. De Roeck, J. R. Ellis and D.Schulte (Editors), *Physics at the CLIC multi-TeV linear collider*, CERN-2004-005 [arXiv:hep-ph/0412251].
[3] N. Sinev *et al.*, Nucl. Instrum. Meth. A **409** (1998) 243.
[4] M. Battaglia, D. Contarato, P. Giubilato, L. Greiner, L. Glesener and B. Hooberman, Nucl. Instrum. Meth. A **579** (2007) 675.
[5] A. Besson *et al.*, Nucl. Instrum. and Meth. A **568** (2006) 233.
[6] Yu. Gornushkin *et al.*, Nucl. Instrum. and Meth. A **513** (2003) 291.
[7] G. Deptuch, Nucl. Instrum. and Meth. A **543** (2005) 537.
[8] Aptek Industries, San Jose, CA 95111, USA.
[9] F. Gaede, T. Behnke, N. Graf and T. Johnson, in the *Proc. of 2003 Conf. for Computing in High-Energy and Nuclear Physics* (CHEP 03), La Jolla, California, 24-28 Mar 2003, pp TUKT001, [arXiv:physics/0306114].
[10] M. Battaglia, Nucl. Instrum. Meth. A **530** 33 (2004).
[11] K. Buesser, *In the Proceedings of 2005 International Linear Collider Workshop (LCWS 2005), Stanford, California, 18-22 Mar 2005, pp 1116.*
[12] F. Gaede, Nucl. Instrum. Meth. A **559** (2006) 177.
[13] S. Agostinelli *et al.*, Nucl. Instrum. Meth. A **506** (2003) 250.
[14] M. Battaglia, Nucl. Instrum. Meth. A **572** (2007) 274.
[15] T. Lohse, Report DESY 95-103.